

## THE ADIABATIC EXPONENT LIMITS OF RIEMANN SOLUTIONS FOR THE EXTENDED MACROSCOPIC PRODUCTION MODEL\*

SHAN SHAN, CHUN SHEN\*\* AND ZHIJIAN WEI

**Abstract.** The exact Riemann solutions for the extended macroscopic production model with an adiabatic exponent are constructed in perfectly explicit forms. The asymptotic limit of Riemann solution consisting of 1-shock wave and 2-contact discontinuity tends to a delta shock solution for the pressureless gas dynamics model under the special over-compressive entropy condition as the adiabatic exponent drops to one. In contrast, the asymptotic limit of Riemann solution composed of 1-rarefaction wave and 2-contact discontinuity tends to the vacuum solution surrounded by two contact discontinuities by letting the adiabatic exponent tend to one, in which the state in the interior of the 1-rarefaction wave fan is developed into vacuum. The intrinsic phenomena of concentration and cavitation are identified and investigated carefully during this limiting process, which displays more complicated and completely different behavior compared with previous literature. In addition, some representative numerical calculations are also provided, which are in well agreement with our theoretical results.

**Mathematics Subject Classification.** 35L65, 35L67, 76N15.

Received March 7, 2022. Accepted June 26, 2022.

### 1. INTRODUCTION

Recently, the 2-order macroscopic production model of data fitting has been introduced originally by Forestier-Coste, Gottlich and Herty [10] in the following form

$$\begin{cases} \rho_t + (\rho u)_x = 0, \\ \left( \rho u(1 + p(\rho)) \right)_t + \left( \rho u^2(1 + p(\rho)) \right)_x = 0, \end{cases} \quad (1.1)$$

where the two non-negative state variables  $u$  and  $\rho$  are served as the product velocity and density separately and the equation of state  $p = p(\rho)$  is usually used to represent the anticipated factor of the production line. More precisely, the model (1.1) was well used to simulate the interactivity between the product density  $\rho$  and the weighted product property  $z = \rho u(1 + p(\rho)) = \rho u + \rho^2 u$  by taking the anticipated factor  $p(\rho) = \rho$  from discrete event simulations according to sampled data. It is of interest to find that the model (1.1) is very reasonable to describe a high-volume multistage production line for the reason that the information propagation speed is

\*This work is partially supported by Shandong Provincial Natural Science Foundation (ZR2019MA058).

*Keywords and phrases:* Riemann problem, macroscopic production model, delta shock wave, vacuum state, adiabatic exponent.  
School of Mathematics and Statistics Science, Ludong University, Yantai, Shandong Province 264025, P.R. China.

\*\* Corresponding author: [shenchun3641@sina.com](mailto:shenchun3641@sina.com)

bounded by the product velocity  $u$  as well as all the emerged hyperbolic waves can travel with non-negative speeds. In addition, it should be pointed out that the variable  $x$  is used to stand for the degree of completion or stage of production.

It is of very interest to notice that the model (1.1) is attributed to the well-known hyperbolic systems of Temple class [6, 42] and thus it has been received extensively attention in the field of hyperbolic conservation laws although the variable  $x$  does not served as a physical position. More specifically, the singular  $\delta$ -standing wave was found by Sun [39] when the Riemann problem for (1.1) was considered under the situation  $p(\rho) = \rho$ . Furthermore, some new exact solutions for (1.1) in the case of  $p(\rho) = \rho$  have also been obtained by Sil and Raja Sekhar [37, 38] with the help of nonclassical symmetry analysis as well as interactions of nonlinear waves have been widely investigated by Minhajul and Raja Sekhar [21]. Very recently, exact Riemann solutions have been obtained and wave interactions have been dealt with carefully in [43] for (1.1) by taking the pressure-density relation  $p(\rho) = -\frac{1}{\rho}$  for Chaplygin gas.

It should be addressed especially that the asymptotic limits  $\varepsilon \rightarrow 0$  of Riemann solutions for the model (1.1) with the perturbed anticipated factor  $p(\rho) = \varepsilon\rho$  have been considered by Zhang and Sun [47]. It is clear to find that the formal limit  $\varepsilon \rightarrow 0$  of the model (1.1) with  $p(\rho) = \varepsilon\rho$  is the well-known pressureless gas dynamics model. However, it was shown in [47] that the limits  $\varepsilon \rightarrow 0$  of Riemann solutions for the model (1.1) associated with  $p(\rho) = \varepsilon\rho$  cannot converge to the corresponding ones for the pressureless gas dynamics model. In order to remedy it, a new perturbed macroscopic production model was also proposed in [47]. It is worthy noticing that the establishment of macroscopic production model was usually to imitate the isentropic gas dynamical Euler model by taking the anticipated factor  $p(\rho) = \rho^{\gamma-1}$  with the requirement  $\gamma \in (1, 2)$ . In fact, it was stressed in [10] that other anticipated factors or clearing functions were of course caused when the proposed procedure was not limited to the assumptions made there and could be extended to other distributions for the serving and arrival process. It was also pointed out in [3] that the kinetic derivation of the macroscopic production model was usually carried out in terms of an adiabatic closure, which motivates us to choose the anticipated factor  $p(\rho) = \rho^{\gamma-1}$  with the requirement  $\gamma \in (1, 2)$  here. In the current work, we will take the anticipated factor  $p(\rho) = \rho^{\gamma-1}$  for the macroscopic production model (1.1), which can be simplified into the form

$$\begin{cases} \rho_t + (\rho u)_x = 0, \\ (\rho u + \rho^\gamma u)_t + (\rho u^2 + \rho^\gamma u^2)_x = 0. \end{cases} \quad (1.2)$$

To be more specific, we shall draw our attention on the Riemann problem for the system (1.2) subject to the following initial condition consisting of two piecewise constant states separated at the origin in the form

$$(\rho, u)(x, 0) = \begin{cases} (\rho_-, u_-), & x < 0, \\ (\rho_+, u_+), & x > 0. \end{cases} \quad (1.3)$$

Actually, it is not difficult to find that the 1-characteristic field is genuinely nonlinear when  $\rho > 0$  and  $u > 0$  or linearly degenerate when  $\rho = 0$  or  $u = 0$  under our assumption  $1 < \gamma < 2$ . On the other hand, the 2-characteristic field is linearly degenerate for ever. As a consequence, if the restrictive conditions  $\rho_\pm > 0$  and  $u_\pm > 0$  are required in (1.3), then the Riemann solution of (1.2)–(1.3) is made up of 1-rarefaction (or 1-shock) wave and 2-contact discontinuity where vacuum may be involved under some suitable initial conditions.

It is of great interest to take into account the influence of the parameter  $\gamma$  on the solutions of the Riemann problem (1.2)–(1.3). It was shown in [24] that the high Mach number limit amounts to the limit  $\gamma \rightarrow 1^+$  for fixed initial total energy in the study of the one-dimensional piston problem for the non-isentropic compressible Euler system of polytropic gas, where the mass concentration at the piston position or the vacuum formation is possibly caused. It is evident to see that if the limit  $\gamma \rightarrow 1^+$  is taken in the system (1.2), then it is formally

transformed into the pressureless gas dynamics model [7, 14, 32] as follows:

$$\begin{cases} \rho_t + (\rho u)_x = 0, \\ (\rho u)_t + (\rho u^2)_x = 0. \end{cases} \quad (1.4)$$

It is well-known nowadays that the system (1.4) is weakly (or non-strictly) hyperbolic and has only a coincident and linearly degenerate eigenvalue. The main feature lies in that the Riemann solution of (1.4)–(1.3) is either a delta shock wave denoted by  $\delta$ -shock for the case  $u_+ < u_-$  or vacuum surrounded by two contact discontinuities for the case  $u_+ > u_-$ . Significantly, the system (1.4) was also adopted in the study of the product flow in connection with queuing networks and supply chains [4, 5], in which it was very effective for slowly changing inflows and was based on the closure hypothesis that was a rare event for each part to overtake each other.

The main aim of this work is concerned with the intrinsic phenomena of concentration and cavitation by sending the limits  $\gamma \rightarrow 1^+$  of Riemann solutions of (1.2)–(1.3). On the one hand, if  $0 < u_+ < u_-$ , then the Riemann solution of (1.2)–(1.3) is made up of 1-shock wave  $S_1$  and 2-contact discontinuity  $J_2$  for any  $\gamma > 1$ . It is found evidently that the front of 1-shock wave  $S_1$  tends to the front of 2-contact discontinuity  $J_2$  at the line  $x = u_+t$  when the limit  $\gamma \rightarrow 1^+$  is taken. Moreover, the concentration phenomenon can be observed clearly due to the fact that the mutual superposition of  $S_1$  and  $J_2$  on the line  $x = u_+t$  gives rise to a  $\delta$ -shock  $S_\delta$  in the limiting  $\gamma \rightarrow 1^+$  situation. It is of interest to find that the strength and wave-speed of  $\delta$ -shock are obviously different from each other between the limit  $\gamma \rightarrow 1^+$  of Riemann solution  $S_1 + J_2$  of (1.2)–(1.3) and the corresponding Riemann solution of (1.4)–(1.3). This is due to the fact that the  $\delta$ -shock solution for the pressureless gas dynamics model (1.4) is usually obtained under the over-compressive  $\delta$ -entropy condition  $u_+ < \sigma_\delta < u_-$ . However, the limit  $\gamma \rightarrow 1^+$  of Riemann solution  $S_1 + J_2$  of (1.2)–(1.3) results in another special over-compressive entropy condition  $u_+ = \tilde{\sigma}_\delta < u_-$  in the marginal situation. In fact, it may not be surprising to find that different perturbations for the pressureless gas dynamics model (1.4) usually produce delta shock waves with different strengths and wave-speeds. On the other hand, if  $0 < u_- < u_+$ , then the Riemann solution of (1.2)–(1.3) is composed of 1-rarefaction wave  $R_1$  and 2-contact discontinuity  $J_2$  with the intermediate non-vacuum constant state when  $u_- < u_+ < 2u_-$  or the vacuum intermediate state when  $u_+ > 2u_-$  by taking  $\gamma - 1 (> 0)$  as our expected smallness. It is very interesting to see that the state in the interior of the 1-rarefaction wave fan  $R_1$  is developed into vacuum in the limiting  $\gamma \rightarrow 1^+$  situation. Furthermore, the limit  $\gamma \rightarrow 1^+$  of Riemann solution of (1.2)–(1.3) is well concurrent with the corresponding vacuum solution surrounded by two contact discontinuities of the Riemann problem (1.4)–(1.3). During the limiting  $\gamma \rightarrow 1^+$  process, the cavitation phenomenon can be well observed and studied in detail, which displays more complicated and completely different behavior compared with previous literature.

To the end, we briefly review some related results about the formation of  $\delta$ -shock wave and vacuum state in the Riemann solutions for the pressureless gas dynamics model (1.4) and also other related models. First of all, the vanishing pressure method was extensively used such as in [8, 11, 12, 22, 26, 30, 33, 41]. Subsequently, the approach of the so-called flux function limit was also adopted such as in [29, 40, 44–46]. Recently, the approach of the adiabatic exponent limit has been well carried out for example in [15, 31, 34–36, 48, 49]. In addition, there are still some other very effective methods [9, 16, 17, 23, 25, 27] to deal with the related problems of  $\delta$ -shocks. Finally, it is necessary to point out that delta shock wave has also been found in other hyperbolic models, such as in the nonlinear chromatography [20], in the shallow water dynamics [18], in the thin film [28] and also in the porous media [13].

The structure of this paper is organized as follows. In Section 2, the Riemann solutions of (1.4) and (1.3) are stated concisely for completeness, which include either  $\delta$ -shock or vacuum state. In Section 3, the fundamental properties and the curves of elementary waves are analyzed at first before all the exact Riemann solutions of (1.2)–(1.3) are constructed in fully explicit forms. In Section 4, the limits  $\gamma \rightarrow 1^+$  of Riemann solutions of (1.2)–(1.3) are analyzed carefully for two different cases. More specifically, if  $0 < u_+ < u_-$ , then the limit  $\gamma \rightarrow 1^+$  of Riemann solution  $S_1 + J_2$  of (1.2)–(1.3) tends to a  $\delta$ -shock solution of (1.4)–(1.3) under the special over-compressive entropy inequality  $u_+ = \tilde{\sigma}_\delta < u_-$  in the marginal situation, which also satisfies the system (1.4) in the weak sense of Schwartz distributions. Otherwise, if  $0 < u_- < u_+$ , then the limit  $\gamma \rightarrow 1^+$  of Riemann

solution  $R_1 + J_2$  of (1.2)–(1.3) also tends to the corresponding vacuum Riemann solution of (1.4)–(1.3). To the end, the numerical calculations are also offered to confirm the formation of  $\delta$ -shock and vacuum in Section 5.

## 2. PRELIMINARIES

In order to facilitate the readers and make the paper self-contained, this section summarizes briefly the results of Riemann solutions for the pressureless gas dynamic system (1.4), please see [7, 8, 32] for a thorough presentation. It is found evidently that (1.4) is a weakly (or non-strictly) hyperbolic system and has only a coincident and linearly degenerate eigenvalue  $\lambda = u$ .

If  $u_- < u_+$ , then the Riemann solution of (1.4)–(1.3) is made up of two contact discontinuities including vacuum state in the middle of the form

$$(\rho, u)(x, t) = \begin{cases} (\rho_-, u_-), & -\infty < x < u_-t, \\ (0, \frac{x}{t}), & u_-t < x < u_+t, \\ (\rho_+, u_+), & u_+t < x < +\infty. \end{cases} \quad (2.1)$$

Otherwise, if  $u_- > u_+$ , then a solution involving a weighted  $\delta$ -measure supported on a curve should be considered. Hence, we need to first introduce the definition of  $\delta$ -measure [8, 16, 32] in order to give a detailed description of  $\delta$ -shock solution of (1.4)–(1.3).

**Definition 2.1.** For each  $\varphi(x, t) \in C_0^\infty(R \times R_+)$ , a weighted Dirac  $\delta$ -function  $\omega(t)\delta_\Gamma$  superimposed upon a smooth curve  $\Gamma = \{(x, t) | x = x(t), 0 \leq t < +\infty\}$  in the  $(x, t)$  plane is given by

$$\langle \omega(t)\delta_\Gamma, \varphi(x, t) \rangle = \int_0^{+\infty} \omega(t)\varphi(x(t), t)dt. \quad (2.2)$$

In view of Definition 2.1, if  $u_- > u_+$ , then we can construct a  $\delta$ -shock solution of (1.4)–(1.3) given by

$$(\rho, u)(x, t) = \begin{cases} (\rho_-, u_-), & x < \sigma_\delta t, \\ (\omega(t)\delta(x - \sigma_\delta t), u_\delta), & x = \sigma_\delta t, \\ (\rho_+, u_+), & x > \sigma_\delta t, \end{cases} \quad (2.3)$$

in which  $\Gamma = \{(\sigma_\delta t, t), 0 \leq t < +\infty\}$ . Actually, the formal solution (2.3) should satisfy

$$\langle \rho, \varphi_t \rangle + \langle \rho u, \varphi_x \rangle = 0, \quad \langle \rho u, \varphi_t \rangle + \langle \rho u^2, \varphi_x \rangle = 0,$$

holding for each  $\varphi(x, t) \in C_0^\infty(R \times R_+)$ , where

$$\langle \rho u^k, \varphi \rangle = \int_0^{+\infty} \int_{-\infty}^{\sigma_\delta t} \rho_- u_-^k \varphi(x, t) dx dt + \int_0^{+\infty} \int_{\sigma_\delta t}^{+\infty} \rho_+ u_+^k \varphi(x, t) dx dt + \langle \omega(t)u_\delta^k \delta_\Gamma, \varphi \rangle,$$

with  $k = 0, 1, 2$ . More specifically, it is obtained that

$$\sigma_\delta = u_\delta = \frac{\sqrt{\rho_+}u_+ + \sqrt{\rho_-}u_-}{\sqrt{\rho_+} + \sqrt{\rho_-}}, \quad \omega(t) = \sqrt{\rho_- \rho_+}(u_- - u_+)t. \quad (2.4)$$

It suffices to show that the  $\delta$ -shock solution (2.3)–(2.4) needs to satisfy the following generalized Rankine-Hugoniot conditions

$$\frac{dx}{dt} = \sigma_\delta, \quad \frac{d\omega(t)}{dt} = \sigma_\delta[\rho] - [\rho u], \quad \frac{d(\omega(t)u_\delta)}{dt} = \sigma_\delta[\rho u] - [\rho u^2], \quad (2.5)$$

in connection with the over-compressive  $\delta$ -entropy inequality  $u_+ < \sigma_\delta < u_-$ .

### 3. CONSTRUCTION OF RIEMANN SOLUTIONS OF (1.2)–(1.3)

The aim of this section is devoted to constructing all the possible solutions of the Riemann problem (1.2)–(1.3). The system (1.2) is adapted conveniently into the following quasi-linear form

$$\begin{pmatrix} 1 & 0 \\ u + \gamma\rho^{\gamma-1}u & \rho + \rho^\gamma \end{pmatrix} \begin{pmatrix} \rho \\ u \end{pmatrix}_t + \begin{pmatrix} u & \rho \\ u^2 + \gamma\rho^{\gamma-1}u^2 & 2\rho u + 2\rho^\gamma u \end{pmatrix} \begin{pmatrix} \rho \\ u \end{pmatrix}_x = \begin{pmatrix} 0 \\ 0 \end{pmatrix}. \quad (3.1)$$

It suffices to get two real and different eigenvalues

$$\lambda_1(\rho, u) = \frac{u(1 + (2 - \gamma)\rho^{\gamma-1})}{1 + \rho^{\gamma-1}}, \quad \lambda_2(\rho, u) = u, \quad (3.2)$$

as well as the associated right eigenvectors

$$\vec{r}_1 = (1 + \rho^{\gamma-1}, (1 - \gamma)\rho^{\gamma-2}u)^T, \quad \vec{r}_2 = (1, 0)^T. \quad (3.3)$$

Moreover, it is shown that

$$\lambda_1 - \lambda_2 = \frac{(1 - \gamma)\rho^{\gamma-1}u}{1 + \rho^{\gamma-1}},$$

such that  $\lambda_1 < \lambda_2$  holds provided that  $u > 0$  and  $\rho > 0$  under our assumption  $1 < \gamma < 2$ . Hence, the system (1.2) is strictly hyperbolic in the interior of quarter  $(\rho, u)$  plane and weakly (or non-strictly) hyperbolic on the positive  $\rho$ -axis or  $u$ -axis. Let  $\nabla = (\frac{\partial}{\partial \rho}, \frac{\partial}{\partial u})$  be the gradient operator, by a trivial and tedious calculation, then we have

$$\nabla \lambda_1 \cdot \vec{r}_1 = \frac{(1 - \gamma)(\gamma + (2 - \gamma)\rho^{\gamma-1})\rho^{\gamma-2}u}{1 + \rho^{\gamma-1}} \neq 0, \quad \nabla \lambda_2 \cdot \vec{r}_2 = 0,$$

holding for  $1 < \gamma < 2$ ,  $u > 0$  and  $\rho > 0$ . The above result shows that the characteristic field of  $\lambda_1$  is genuinely nonlinear and the characteristic field of  $\lambda_2$  is always linearly degenerate in the interior of the quarter  $(\rho, u)$  plane, which implies that  $\lambda_1$  corresponds to shock or rarefaction wave and  $\lambda_2$  corresponds to contact discontinuity.

The rarefaction curve is firstly studied. Since the Riemann problem (1.2)–(1.3) remains unchanged under uniform stretching, the following form of transformation is carried out to find self-similar solutions

$$(\rho, u)(x, t) = (\rho, u)(\xi), \quad \xi = \frac{x}{t}.$$

Thus, we can convert the Riemann problem (1.2)–(1.3) into the boundary value problem of the following form

$$\begin{cases} -\xi\rho_\xi + (\rho u)_\xi = 0, \\ -\xi(\rho u + \rho^\gamma u)_\xi + (\rho u^2 + \rho^\gamma u^2)_\xi = 0, \\ (\rho, u)(\pm\infty) = (\rho_\pm, u_\pm), \end{cases} \quad (3.4)$$

which allows us to get

$$\begin{pmatrix} u - \xi & \rho \\ (1 + \gamma\rho^{\gamma-1})(u - \xi)u & \rho(1 + \rho^{\gamma-1})(2u - \xi) \end{pmatrix} \begin{pmatrix} \rho \\ u \end{pmatrix}_\xi = \begin{pmatrix} 0 \\ 0 \end{pmatrix}. \quad (3.5)$$

For a given left state  $(\rho_-, u_-)$  in the interior of the quarter  $(\rho, u)$  plane, by using the standard process and with the help of  $\lambda_1(\rho, u) > \lambda_1(\rho_-, u_-)$ , the 1-rarefaction curve may be represented concisely as

$$R_1(\rho_-, u_-) : \xi = \lambda_1(\rho, u) = \frac{(1 + (2 - \gamma)\rho^{\gamma-1})u}{1 + \rho^{\gamma-1}}, \quad (1 + \rho^{\gamma-1})u = (1 + \rho_-^{\gamma-1})u_-, \quad \rho < \rho_-, \quad u > u_-. \quad (3.6)$$

It can be obtained that

$$\begin{aligned} \frac{du}{d\rho} &= -\frac{(\gamma - 1)(1 + \rho_-^{\gamma-1})u_- \rho^{\gamma-2}}{(1 + \rho^{\gamma-1})^2} < 0, \\ \frac{d^2u}{d\rho^2} &= \frac{(\gamma - 1)(1 + \rho_-^{\gamma-1})u_-(\gamma\rho^{2\gamma-4} - (\gamma - 2)\rho^{\gamma-3})}{(1 + \rho^{\gamma-1})^3} > 0, \end{aligned}$$

which permits us to find that the curve  $R_1(\rho_-, u_-)$  is convex in the quarter  $(\rho, u)$  plane. In addition, it is obvious to find that the curve  $R_1(\rho_-, u_-)$  and the positive  $u$ -axis intersect at the point  $(0, u_-(1 + \rho_-^{\gamma-1}))$ .

It is quite natural to consider the discontinuous curve now, then the Rankine-Hugoniot jump conditions are written as

$$\sigma[\rho] = [\rho u], \quad \sigma[\rho u + \rho^\gamma u] = [\rho u^2 + \rho^\gamma u^2]. \quad (3.7)$$

where  $\sigma = \frac{dx}{dt}$  is the wave-speed of the discontinuity and  $[q] = q - q_-$  represents the jump of the quantity  $q$  passing through the discontinuity. If  $\sigma = 0$ , then the solution  $(\rho, u) = (\rho_-, u_-)$  is a trivial constant state. Otherwise, if  $\sigma \neq 0$ , then we obtain

$$[\rho u][\rho u + \rho^\gamma u] = [\rho][\rho u^2 + \rho^\gamma u^2].$$

which gives

$$\rho\rho_- \left( (\rho_-^{\gamma-1} + 1)u_- - (\rho^{\gamma-1} + 1)u \right) (u - u_-) = 0. \quad (3.8)$$

If  $u \neq u_-$ , by using the classical Lax entropy condition, then the 1-shock curve follows from (3.8) clearly that

$$S_1(\rho_-, u_-) : \sigma_1 = \frac{\rho u - \rho_- u_-}{\rho - \rho_-}, \quad (1 + \rho^{\gamma-1})u = (1 + \rho_-^{\gamma-1})u_-, \quad \rho > \rho_-, \quad u < u_-. \quad (3.9)$$

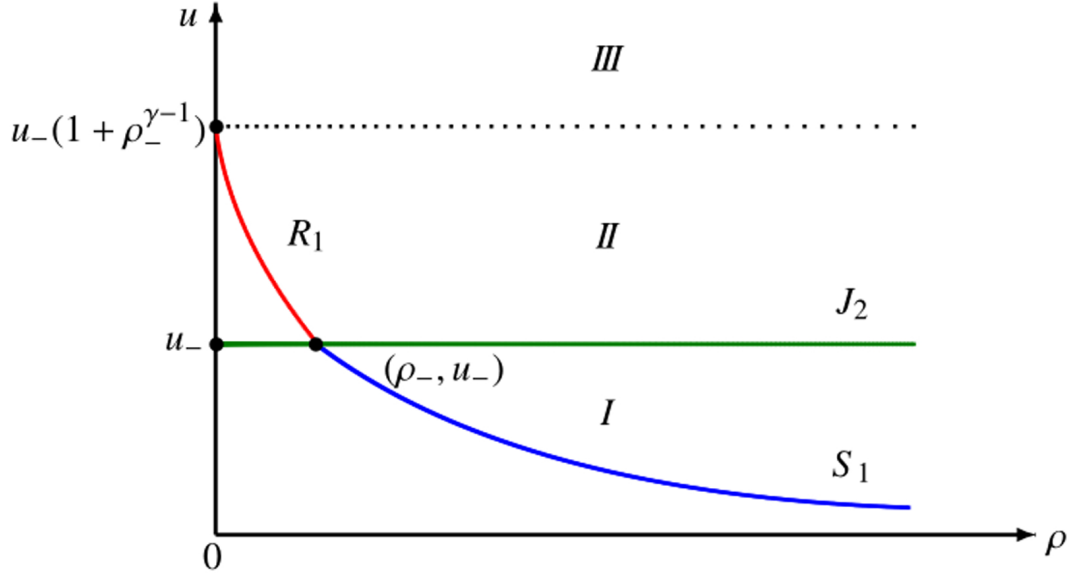


FIGURE 1. Let the left state  $(\rho_-, u_-)$  be fixed in the interior of quarter  $(\rho, u)$  plane, then the Riemann solution of (1.2)–(1.3) can be constructed uniquely according to the right state  $(\rho_+, u_+)$  in the different regions *I*, *II* and *III*.

It is evident to find from (3.9) that the curve  $S_1(\rho_-, u_-)$  regards the positive  $\rho$ -axis as its asymptotic line in the quarter  $(\rho, u)$  plane. It is also known obviously that the expressions of shock and rarefaction curves are exactly the same, thus the system (1.2) belongs to the famous Temple-type [6, 42]. Otherwise, if  $u = u_-$ , then the curve of 2-contact discontinuity is obtained immediately that

$$J_2(\rho_-, u_-) : \tau_2 = u = u_-. \quad (3.10)$$

It can be easily analyzed from Figure 1 that the quarter  $(\rho, u)$  phase plane is divided into three parts by the 1-rarefaction curve  $R_1(\rho_-, u_-)$ , the 1-shock curve  $S_1(\rho_-, u_-)$  and the curve of 2-contact discontinuity  $J_2(\rho_-, u_-)$ . As a consequence, the Riemann solutions of (1.2) and (1.3) can be represented as the usual notations  $S_1 + J_2$ ,  $R_1 + J_2$  and  $R_1 + Vac + J_2$  when the right state  $(\rho_+, u_+)$  varies from bottom to top in the quarter  $(\rho, u)$  phase plane.

- (1) If  $0 < u_+ < u_-$ , then  $(\rho_+, u_+)$  falls in the region *I* and the Riemann solution of (1.2)–(1.3) can be expressed as

$$(\rho, u)(x, t) = \begin{cases} (\rho_-, u_-), & -\infty < \frac{x}{t} < \sigma_1, \\ (\rho_*, u_+), & \sigma_1 < \frac{x}{t} < \tau_2, \\ (\rho_+, u_+), & \tau_2 < \frac{x}{t} < +\infty, \end{cases} \quad (3.11)$$

where  $\rho_*$  is calculated by

$$u_+(1 + \rho_*^{\gamma-1}) = u_-(1 + \rho_-^{\gamma-1}), \quad (3.12)$$

namely

$$\rho_* = \left( \frac{(1 + \rho_-^{\gamma-1})u_- - u_+}{u_+} \right)^{\frac{1}{\gamma-1}}. \quad (3.13)$$

Additionally, the wave-speeds of 1-shock wave  $S_1$  and 2-contact discontinuity  $J_2$  are given respectively by

$$\sigma_1 = \frac{\rho_* u_+ - \rho_- u_-}{\rho_* - \rho_-}, \quad \tau_2 = u_+. \quad (3.14)$$

- (2) If  $u_- < u_+ < u_-(1 + \rho_-^{\gamma-1})$ , then  $(\rho_+, u_+)$  is situated in the region  $II$  and the Riemann solution of (1.2)–(1.3) can be written as

$$(\rho, u)(x, t) = \begin{cases} (\rho_-, u_-), & -\infty < \frac{x}{t} < \lambda_1(\rho_-, u_-), \\ (\rho, u), & \lambda_1(\rho_-, u_-) \leq \frac{x}{t} \leq \lambda_1(\rho_*, u_+), \\ (\rho_*, u_+), & \lambda_1(\rho_*, u_+) < \frac{x}{t} < \tau_2, \\ (\rho_+, u_+), & \tau_2 < \frac{x}{t} < +\infty, \end{cases} \quad (3.15)$$

where  $\rho_*$  is also calculated by (3.12) and given by (3.13) due to the feature of Temple-type. In addition, the state  $(\rho, u)$  in the wave fan of  $R_1$  changes from  $(\rho_-, u_-)$  to  $(\rho_*, u_+)$ , which is uniquely determined by

$$(1 + \rho^{\gamma-1})u = (1 + \rho_-^{\gamma-1})u_-, \quad \xi = \frac{x}{t} = \frac{(1 + (2 - \gamma)\rho^{\gamma-1})u}{1 + \rho^{\gamma-1}}. \quad (3.16)$$

For convenience, we use the notation  $\bar{u} = u_-(1 + \rho_-^{\gamma-1})$  and then we further get

$$\begin{cases} \rho = \left( \frac{(2 - \gamma)\bar{u} - 2\xi + \sqrt{(2 - \gamma)^2 \bar{u}^2 + 4(\gamma - 1)\xi\bar{u}}}{2\xi} \right)^{\frac{1}{\gamma-1}}, \\ u = \frac{(\gamma - 2)\bar{u} + \sqrt{(2 - \gamma)^2 \bar{u}^2 + 4(\gamma - 1)\xi\bar{u}}}{2(\gamma - 1)}. \end{cases} \quad (3.17)$$

Accordingly, the wave-speed of  $J_2$  is also  $\tau_2 = u_+$  as well as the wave-back and the wave-front of  $R_1$  are computed respectively by

$$\lambda_1(\rho_-, u_-) = \frac{(1 + (2 - \gamma)\rho_-^{\gamma-1})u_-}{1 + \rho_-^{\gamma-1}}, \quad \lambda_1(\rho_*, u_+) = \frac{(1 + (2 - \gamma)\rho_*^{\gamma-1})u_+}{1 + \rho_*^{\gamma-1}}. \quad (3.18)$$

(3) Finally, if  $u_+ > u_-(1 + \rho_-^{\gamma-1})$ , then  $(\rho_+, u_+)$  is located in the region *III* and the Riemann solution of (1.2)–(1.3) is represented by

$$(\rho, u)(x, t) = \begin{cases} (\rho_-, u_-), & -\infty < \frac{x}{t} < \lambda_1(\rho_-, u_-), \\ (\rho, u), & \lambda_1(\rho_-, u_-) \leq \frac{x}{t} \leq \lambda_1(0, \bar{u}), \\ vac, & \lambda_1(0, \bar{u}) < \frac{x}{t} < \tau_2, \\ (\rho_+, u_+), & \tau_2 < \frac{x}{t} < +\infty. \end{cases} \quad (3.19)$$

In the formula (3.19), the varying state variable  $(\rho, u)$  in the wave fan of  $R_1$  is also given by (3.17), the wave-speed of  $J_2$  is still  $\tau_2 = u_+$ , and the wave-front of  $R_1$  is also given by the first relation of (3.18) but now the wave-back of  $R_1$  is given by  $\lambda_1(0, \bar{u}) = \bar{u}$ .

As a consequence, we have constructed three different structures of Riemann solutions of (1.2)–(1.3) according to the ordering relations  $0 < u_+ < u_-$ ,  $u_- < u_+ < u_-(1 + \rho_-^{\gamma-1})$  and  $u_+ > u_-(1 + \rho_-^{\gamma-1})$ . In the remaining content, it is of interest to consider the limiting behavior of Riemann solution of (1.2)–(1.3) as  $u_+ \rightarrow 0^+$ . For each fixed  $\gamma \in (1, 2)$ , sending the limit  $u_+ \rightarrow 0^+$  in (3.13) immediately gives

$$\lim_{u_+ \rightarrow 0^+} \rho_* = \lim_{u_+ \rightarrow 0^+} \left( \frac{(1 + \rho_-^{\gamma-1})u_- - u_+}{u_+} \right)^{\frac{1}{\gamma-1}} = +\infty. \quad (3.20)$$

Moreover, it also follows from (3.14) that

$$\lim_{u_+ \rightarrow 0^+} \sigma_1 = \lim_{u_+ \rightarrow 0^+} \frac{\rho_* u_+ - \rho_- u_-}{\rho_* - \rho_-} = 0, \quad \lim_{u_+ \rightarrow 0^+} \tau_2 = \lim_{u_+ \rightarrow 0^+} u_+ = 0, \quad (3.21)$$

which implies that the 1-shock wave  $S_1$  and the 2-contact discontinuity  $J_2$  coincide with each other at the line  $x = 0$  in the  $(x, t)$  plane to form a so-called delta standing wave when the limit  $u_+ \rightarrow 0^+$  is taken. It is necessary to compute the total quantity of  $\rho$  between  $S_1$  and  $J_2$  in the limiting  $u_+ \rightarrow 0^+$  circumstance as follows:

$$\lim_{u_+ \rightarrow 0^+} \int_{\sigma_1-0}^{\tau_2+0} \rho_* d\xi = \lim_{u_+ \rightarrow 0^+} \int_{\frac{\rho_* u_+ - \rho_- u_-}{\rho_* - \rho_-} - 0}^{u_+ + 0} \left( \frac{(1 + \rho_-^{\gamma-1})u_- - u_+}{u_+} \right)^{\frac{1}{\gamma-1}} d\xi.$$

Integrating the first equation in (3.4) with respect to  $\xi$  from  $\sigma_1 - 0$  to  $\tau_2 + 0$  leads to

$$\int_{\sigma_1-0}^{\tau_2+0} -\xi d\rho + d(\rho u) = -\xi \rho \Big|_{\sigma_1-0}^{\tau_2+0} + \int_{\sigma_1-0}^{\tau_2+0} \rho d\xi + \rho u \Big|_{\sigma_1-0}^{\tau_2+0} = 0,$$

which gives

$$\int_{\sigma_1-0}^{\tau_2+0} \rho_* d\xi = \tau_2 \rho_+ - \sigma_1 \rho_- - \rho_+ u_+ + \rho_- u_-.$$

Thanks to (3.21), one can arrive at

$$\lim_{u_+ \rightarrow 0^+} \int_{\sigma_1 t - 0}^{\tau_2 t + 0} \rho_* d\xi = \rho_- u_- \quad \text{and further} \quad \lim_{u_+ \rightarrow 0^+} \int_{\sigma_1 t - 0}^{\tau_2 t + 0} \rho_* dx = \rho_- u_- t, \quad (3.22)$$

which indicates that the singularity occurs for the density  $\rho$  with a weighted Dirac delta function at the position  $x = 0$  when  $u_+ = 0$ . Motivated by [8, 32], for the special case  $u_+ = 0$ , the Riemann problem (1.2)–(1.3) admits a delta standing wave solution in the form

$$\rho(x, t) = \begin{cases} \rho_-, & x < 0, \\ \rho_- u_- t \delta(x), & x = 0, \\ \rho_+, & x > 0, \end{cases} \quad u(x, t) = \begin{cases} u_-, & x < 0, \\ 0, & x > 0. \end{cases} \quad (3.23)$$

Moreover, we further have

$$\lambda_1(\rho_+, 0) = \lambda_2(\rho_+, 0) = 0 < \lambda_1(\rho_-, u_-) < \lambda_2(\rho_-, u_-),$$

which indicates that the characteristics on the right-hand side are parallel to the front of delta standing wave as well as the characteristics on the left-hand side break into the front of delta standing wave. Thus, the mass concentration on the front of delta standing wave only comes from the particles on the left-hand side.

#### 4. THE LIMITING BEHAVIOR OF RIEMANN SOLUTIONS OF (1.2)–(1.3) AS $\gamma \rightarrow 1^+$

In this section, we shall discuss the limits of Riemann solutions of (1.2)–(1.3) as  $\gamma \rightarrow 1^+$ . More precisely, our discussion will be divided into two parts according to the ordering relation between  $u_-$  and  $u_+$ .

When  $0 < u_+ < u_-$ , it is shown that the Riemann solution of (1.2)–(1.3) is made up of 1-shock wave  $S_1$  and 2-contact discontinuity  $J_2$  for any  $\gamma > 1$  (see Fig. 2a). It is easy to know from (3.11) that  $(\rho_-, u_-)$  and  $(\rho_*, u_+)$  are connected by 1-shock wave at the velocity  $\sigma_1$ , and  $(\rho_*, u_+)$  and  $(\rho_+, u_+)$  are connected by 2-contact discontinuity at the velocity  $\tau_2$ . Sending the limit  $\gamma \rightarrow 1^+$  in (3.12) immediately leads to

$$\lim_{\gamma \rightarrow 1^+} \rho_*^{\gamma-1} = \frac{2u_- - u_+}{u_+}. \quad (4.1)$$

It suffices to obtain  $\frac{2u_- - u_+}{u_+} > 1$  from the requirement  $0 < u_+ < u_-$ . In view of the limiting relation  $\lim_{\gamma \rightarrow 1^+} \frac{1}{\gamma-1} = +\infty$ , it also follows from (4.1) that

$$\lim_{\gamma \rightarrow 1^+} \rho_* = \lim_{\gamma \rightarrow 1^+} \left( \frac{2u_- - u_+}{u_+} \right)^{\frac{1}{\gamma-1}} = +\infty. \quad (4.2)$$

Taking into account (4.2), it can be derived obviously from (3.14) that

$$\lim_{\gamma \rightarrow 1^+} \sigma_1 = \lim_{\gamma \rightarrow 1^+} \frac{\rho_* u_+ - \rho_- u_-}{\rho_* - \rho_-} = \lim_{\gamma \rightarrow 1^+} \left( u_+ + \frac{\rho_- (u_+ - u_-)}{\rho_* - \rho_-} \right) = u_+ = \lim_{\gamma \rightarrow 1^+} \tau_2, \quad (4.3)$$

which indicates that  $S_1$  and  $J_2$  coincide on the line  $x = u_+ t$  in the limiting  $\gamma \rightarrow 1^+$  situation (see Fig. 2b).

Let us use Lemma 4.1 to describe the formation of singularity at the position  $x = u_+ t$  in the limiting behavior of Riemann solution of (1.2)–(1.3) as  $\gamma \rightarrow 1^+$  for the case  $0 < u_+ < u_-$ .

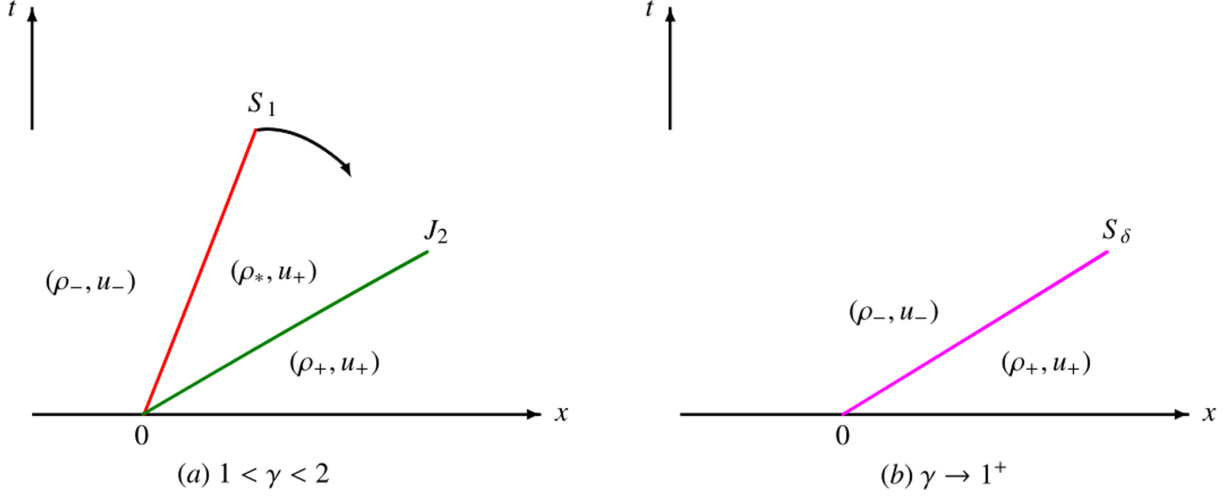


FIGURE 2. In the case of  $0 < u_+ < u_-$ , the Riemann solution  $S_1 + J_2$  of (1.2)–(1.3) is shown on the left-hand side and the corresponding limit  $\gamma \rightarrow 1^+$  of this solution is displayed on the right-hand side.

**Lemma 4.1.** *Let us denote  $\tilde{\sigma}_\delta = u_+$ , then the limiting relations are indicated as follows:*

$$\lim_{\gamma \rightarrow 1^+} (\tau_2 - \sigma_1)\rho_* = \rho_-(u_- - u_+) = \tilde{\sigma}_\delta[\rho] - [\rho u], \quad (4.4)$$

$$\lim_{\gamma \rightarrow 1^+} (\tau_2 - \sigma_1)(\rho_* u_* + \rho_*^\gamma u_*) = 2\rho_- u_-(u_- - u_+) = 2(\tilde{\sigma}_\delta[\rho u] - [\rho u^2]), \quad (4.5)$$

in which  $[q] = q_+ - q_-$  denotes the jump quantity of  $q$  across the discontinuity, etc.

*Proof.* It can be deduced from (3.14) together with (4.2) that

$$\lim_{\gamma \rightarrow 1^+} (\tau_2 - \sigma_1)\rho_* = \lim_{\gamma \rightarrow 1^+} \left( u_+ - \frac{\rho_* u_+ - \rho_- u_-}{\rho_* - \rho_-} \right) \rho_* = \lim_{\gamma \rightarrow 1^+} \frac{\rho_* \rho_- (u_- - u_+)}{\rho_* - \rho_-} = \rho_-(u_- - u_+) = \tilde{\sigma}_\delta[\rho] - [\rho u]. \quad (4.6)$$

Carrying out the Rankine-Hugoniot conditions on  $S_1$  and  $J_2$  for the second equation of (1.2) allows us to arrive at

$$\begin{cases} \sigma_1(\rho_* u_+ + \rho_*^\gamma u_+ - \rho_- u_- - \rho_-^\gamma u_-) = \rho_* u_+^2 + \rho_*^\gamma u_+^2 - \rho_- u_-^2 - \rho_-^\gamma u_-^2, \\ \tau_2(\rho_+ u_+ + \rho_+^\gamma u_+ - \rho_* u_+ - \rho_*^\gamma u_+) = \rho_+ u_+^2 + \rho_+^\gamma u_+^2 - \rho_* u_+^2 - \rho_*^\gamma u_+^2, \end{cases}$$

which immediately gives

$$\begin{aligned}
\lim_{\gamma \rightarrow 1^+} (\tau_2 - \sigma_1)(\rho_* u_+ + \rho_*^\gamma u_+) &= \lim_{\gamma \rightarrow 1^+} (\tau_2 \rho_+ u_+ + \tau_2 \rho_+^\gamma u_+ - \sigma_1 \rho_- u_- - \sigma_1 \rho_-^\gamma u_- \\
&\quad + \rho_- u_-^2 + \rho_-^\gamma u_-^2 - \rho_+ u_+^2 - \rho_+^\gamma u_+^2) \\
&= 2\tilde{\sigma}_\delta \rho_+ u_+ - 2\tilde{\sigma}_\delta \rho_- u_- + 2\rho_- u_-^2 - 2\rho_+ u_+^2 \\
&= 2\rho_- u_- (u_- - u_+) \\
&= 2(\tilde{\sigma}_\delta [\rho u] - [\rho u^2]).
\end{aligned}$$

Moreover, we further have

$$\lim_{\gamma \rightarrow 1^+} (\tau_2 - \sigma_1) \rho_* u_+ = \lim_{\gamma \rightarrow 1^+} \left( u_+ - \frac{\rho_* u_+ - \rho_- u_-}{\rho_* - \rho_-} \right) \rho_* u_+ = \rho_- u_+ (u_- - u_+), \quad (4.7)$$

$$\lim_{\gamma \rightarrow 1^+} (\tau_2 - \sigma_1) \rho_*^\gamma u_+ = \lim_{\gamma \rightarrow 1^+} (\tau_2 - \sigma_1) \rho_* u_+ \cdot \lim_{\gamma \rightarrow 1^+} \rho_*^{\gamma-1} = \rho_- (u_- - u_+) (2u_- - u_+), \quad (4.8)$$

in which the limiting relation (4.2) has been used. The proof is accomplished.  $\square$

In the case of  $0 < u_+ < u_-$ , it can be concluded from the above discussion that the mutual superposition of  $S_1$  and  $J_2$  on the line  $x = u_+ t$  leads to a  $\delta$ -shock  $S_\delta$  in the limiting  $\gamma \rightarrow 1^+$  situation. According to the formula (4.4), let us calculate the strength of  $\delta$ -shock obtained from the limit  $\gamma \rightarrow 1^+$  of Riemann solution  $S_1 + J_2$  of (1.2)–(1.3) as follows:

$$\tilde{\alpha}_\delta(t) = \lim_{\gamma \rightarrow 1^+} \int_{\sigma_1 t}^{\tau_2 t} \rho_* dx = \lim_{\gamma \rightarrow 1^+} \rho_* (\tau_2 t - \sigma_1 t) = (\tilde{\sigma}_\delta [\rho] - [\rho u]) t = \rho_- (u_- - u_+) t. \quad (4.9)$$

In conclusion, for the case  $0 < u_+ < u_-$ , such  $\delta$ -shock solution derived from the limit  $\gamma \rightarrow 1^+$  of Riemann solution  $S_1 + J_2$  of (1.2)–(1.3) can be written as

$$\rho(x, t) = \begin{cases} \rho_-, & x < u_+ t, \\ \tilde{\alpha}_\delta(t) \delta(x - u_+ t), & x = u_+ t, \\ \rho_+, & x > u_+ t, \end{cases} \quad u(x, t) = \begin{cases} u_-, & x < u_+ t, \\ u_+, & x > u_+ t. \end{cases} \quad (4.10)$$

It is sufficient to find from (2.3)–(2.4) and (4.9)–(4.10) that the strength and wave-speed of  $\delta$ -shock are obviously different from each other. This is due to the fact that the  $\delta$ -shock solution (2.3)–(2.4) for the pressureless gas dynamics model (1.4) is obtained under the over-compressive  $\delta$ -entropy inequality  $u_+ < \sigma_\delta < u_-$ . It should be stressed that taking the limit  $\gamma \rightarrow 1^+$  of Riemann solution  $S_1 + J_2$  of (1.2)–(1.3) here leads to another special over-compressive entropy inequality  $u_+ = \tilde{\sigma}_\delta < u_-$  in the marginal situation. Actually, it is probably not a surprise to find that different perturbations for the pressureless gas dynamics model (1.4) may usually give rise to different strengths and wave-speeds of  $\delta$ -shocks [47]. In order to prove rigorously that such  $\delta$ -shock solution (4.10) in connection with (4.9) satisfies the system (1.4) in the weak sense of Schwartz distributions, one of the correct and effective ways is to use a suitable space such as Borel measure, make multiplications in densities and fluxes there, and then map the obtained products into the space of Schwartz distributions and differentiate, which is not the content of the current work and thus omitted here.

**Theorem 4.2.** *Suppose that the Riemann solution of (1.2)–(1.3) consists of a 1-shock wave  $S_1$  and a 2-contact discontinuity  $J_2$  when  $u_+ < u_-$  and  $1 < \gamma < 2$ , then the limit  $\gamma \rightarrow 1^+$  of Riemann solution  $S_1 + J_2$  tends to a  $\delta$ -shock solution (4.10) associated with (4.9) in the sense of distributions. More specifically, the following two weak limiting relations hold that*

$$\lim_{\gamma \rightarrow 1^+} \rho = \rho_- + (\rho_+ - \rho_-)H(x - u_+t) + \rho_-(u_- - u_+)t\delta(x - u_+t), \quad (4.11)$$

$$\lim_{\gamma \rightarrow 1^+} (\rho u + \rho^\gamma u) = 2\rho_-u_- + 2(\rho_+u_+ - \rho_-u_-)H(x - u_+t) + 2\rho_-u_-(u_- - u_+)t\delta(x - u_+t). \quad (4.12)$$

*Proof.* Under our assumptions, the Riemann solution  $S_1 + J_2$  of (1.2)–(1.3) can be represented exactly as the formula (3.11), which satisfies the weak sense of the model (1.2) as follows:

$$\int_{-\infty}^{+\infty} \rho(\xi)(\xi - u(\xi))\varphi'(\xi)d\xi + \int_{-\infty}^{+\infty} \rho(\xi)\varphi(\xi)d\xi = 0, \quad (4.13)$$

$$\int_{-\infty}^{+\infty} (1 + \rho^{\gamma-1}(\xi))\rho(\xi)u(\xi)(\xi - u(\xi))\varphi'(\xi)d\xi + \int_{-\infty}^{+\infty} (1 + \rho^{\gamma-1}(\xi))\rho(\xi)u(\xi)\varphi(\xi)d\xi = 0, \quad (4.14)$$

holding for each  $\varphi(\xi) \in C_0^\infty(-\infty, +\infty)$ .

Let us draw our attention on (4.14), whose first term can be divided into

$$\int_{-\infty}^{+\infty} (1 + \rho^{\gamma-1}(\xi))\rho(\xi)u(\xi)(\xi - u(\xi))\varphi'(\xi)d\xi = \left( \int_{-\infty}^{\sigma_1} + \int_{\sigma_1}^{\tau_2} + \int_{\tau_2}^{+\infty} \right) (1 + \rho^{\gamma-1}(\xi))\rho(\xi)u(\xi)(\xi - u(\xi))\varphi'(\xi)d\xi. \quad (4.15)$$

Sending the limit  $\gamma \rightarrow 1^+$  in the first and last integrals on the right-hand side of (4.15) immediately gives

$$\begin{aligned} & \lim_{\gamma \rightarrow 1^+} \left( \int_{-\infty}^{\sigma_1} + \int_{\tau_2}^{+\infty} \right) (1 + \rho^{\gamma-1}(\xi))\rho(\xi)u(\xi)(\xi - u(\xi))\varphi'(\xi)d\xi \\ &= \lim_{\gamma \rightarrow 1^+} \int_{-\infty}^{\sigma_1} (1 + \rho_-^{\gamma-1})\rho_-u_-(\xi - u_-)\varphi'(\xi)d\xi + \lim_{\gamma \rightarrow 1^+} \int_{\tau_2}^{+\infty} (1 + \rho_+^{\gamma-1})\rho_+u_+(\xi - u_+)\varphi'(\xi)d\xi \\ &= \lim_{\gamma \rightarrow 1^+} \left( (1 + \rho_-^{\gamma-1})\rho_-u_-\sigma_1\varphi(\sigma_1) - (1 + \rho_-^{\gamma-1})\rho_-u_-^2\varphi(\sigma_1) - (1 + \rho_+^{\gamma-1})\rho_+u_+\tau_2\varphi(\tau_2) + (1 + \rho_+^{\gamma-1})\rho_+u_+^2\varphi(\tau_2) \right. \\ & \quad \left. - (1 + \rho_-^{\gamma-1})\rho_-u_- \int_{-\infty}^{\sigma_1} \varphi(\xi)d\xi - (1 + \rho_+^{\gamma-1})\rho_+u_+ \int_{\tau_2}^{+\infty} \varphi(\xi)d\xi \right) \\ &= 2\rho_-u_-(u_- - u_+)\varphi(u_+) - 2 \int_{-\infty}^{+\infty} (\rho_-u_- + (\rho_+u_+ - \rho_-u_-)H(\xi - u_+))\varphi(\xi)d\xi, \end{aligned}$$

in which  $\lim_{\gamma \rightarrow 1^+} \sigma_1 = u_+$  and  $\tau_2 = u_+$  have been used. Thanks to (4.5), passing to the limit  $\gamma \rightarrow 1^+$  in the second integral on the right-hand side of (4.15) leads to

$$\begin{aligned}
& \lim_{\gamma \rightarrow 1^+} \int_{\sigma_1}^{\tau_2} (1 + \rho^{\gamma-1}(\xi)) \rho(\xi) u(\xi) (\xi - u(\xi)) \varphi'(\xi) d\xi \\
&= \lim_{\gamma \rightarrow 1^+} \int_{\sigma_1}^{u_+} (1 + \rho_*^{\gamma-1}) \rho_* u_+ (\xi - u_+) \varphi'(\xi) d\xi \\
&= \lim_{\gamma \rightarrow 1^+} (1 + \rho_*^{\gamma-1}) \rho_* u_+ (u_+ - \sigma_1) \left( \varphi(\sigma_1) - \frac{1}{u_+ - \sigma_1} \int_{\sigma_1}^{u_+} \varphi(\xi) d\xi \right) \\
&= 2\rho_- u_- (u_- - u_+) (\varphi(u_+) - \varphi(u_-)) = 0.
\end{aligned}$$

In summary, it can be concluded from (4.14) that

$$\lim_{\gamma \rightarrow 1^+} \int_{-\infty}^{+\infty} \left( (1 + \rho^{\gamma-1}(\xi)) \rho(\xi) u(\xi) - 2(\rho_- u_- + (\rho_+ u_+ - \rho_- u_-) H(\xi - u_+)) \right) \varphi(\xi) d\xi = 2\rho_- u_- (u_- - u_+) \varphi(u_+). \quad (4.16)$$

In addition, in terms of the formulae (4.7) and (4.8), it also holds that

$$\begin{aligned}
& \lim_{\gamma \rightarrow 1^+} \int_{-\infty}^{+\infty} \rho(\xi) u(\xi) \varphi(\xi) d\xi = \lim_{\gamma \rightarrow 1^+} \left( \int_{-\infty}^{\sigma_1} + \int_{\sigma_1}^{\tau_2} + \int_{\tau_2}^{+\infty} \right) \rho(\xi) u(\xi) \varphi(\xi) d\xi \\
&= \lim_{\gamma \rightarrow 1^+} \left\{ \int_{-\infty}^{\sigma_1} \rho_- u_- \varphi(\xi) d\xi + \int_{\tau_2}^{+\infty} \rho_+ u_+ \varphi(\xi) d\xi + \int_{\sigma_1}^{\tau_2} \rho_* u_+ \varphi(\xi) d\xi \right\} \\
&= \rho_- u_- \int_{-\infty}^{u_+} \varphi(\xi) d\xi + \rho_+ u_+ \int_{u_+}^{+\infty} \varphi(\xi) d\xi + \lim_{\gamma \rightarrow 1^+} (\tau_2 - \sigma_1) \rho_* u_+ \cdot \lim_{\gamma \rightarrow 1^+} \left( \frac{1}{\tau_2 - \sigma_1} \int_{\sigma_1}^{\tau_2} \varphi(\xi) d\xi \right) \\
&= \int_{-\infty}^{+\infty} (\rho_- u_- + (\rho_+ u_+ - \rho_- u_-) H(\xi - u_+)) \varphi(\xi) d\xi + \rho_- u_+ (u_- - u_+) \varphi(u_+),
\end{aligned}$$

and

$$\begin{aligned}
& \lim_{\gamma \rightarrow 1^+} \int_{-\infty}^{+\infty} \rho^\gamma(\xi) u(\xi) \varphi(\xi) d\xi = \lim_{\gamma \rightarrow 1^+} \left( \int_{-\infty}^{\sigma_1} + \int_{\sigma_1}^{\tau_2} + \int_{\tau_2}^{+\infty} \right) \rho^\gamma(\xi) u(\xi) \varphi(\xi) d\xi \\
&= \lim_{\gamma \rightarrow 1^+} \left\{ \int_{-\infty}^{\sigma_1} \rho_-^\gamma u_- \varphi(\xi) d\xi + \int_{\tau_2}^{+\infty} \rho_+^\gamma u_+ \varphi(\xi) d\xi + \int_{\sigma_1}^{\tau_2} \rho_*^\gamma u_+ \varphi(\xi) d\xi \right\} \\
&= \rho_- u_- \int_{-\infty}^{u_+} \varphi(\xi) d\xi + \rho_+ u_+ \int_{u_+}^{+\infty} \varphi(\xi) d\xi + \lim_{\gamma \rightarrow 1^+} (\tau_2 - \sigma_1) \rho_*^\gamma u_+ \cdot \lim_{\gamma \rightarrow 1^+} \left( \frac{1}{\tau_2 - \sigma_1} \int_{\sigma_1}^{\tau_2} \varphi(\xi) d\xi \right) \\
&= \int_{-\infty}^{+\infty} (\rho_- u_- + (\rho_+ u_+ - \rho_- u_-) H(\xi - u_+)) \varphi(\xi) d\xi + \rho_- (u_- - u_+) (2u_- - u_+) \varphi(u_+).
\end{aligned}$$

Performing the same procedure on (4.13) as before gives rise to

$$\lim_{\gamma \rightarrow 1^+} \int_{-\infty}^{+\infty} (\rho(\xi) - \rho_- + (\rho_+ - \rho_-) H(\xi - u_+)) \varphi(\xi) d\xi = \rho_- (u_- - u_+) \varphi(u_+). \quad (4.17)$$

It is desired to obtain the limits  $\gamma \rightarrow 1^+$  of  $\rho$  and  $\rho u + \rho^\gamma u$ . Let  $\psi(x, t) \in C_0^\infty(R \times R_+)$ , taking into account  $\xi = \frac{x}{t}$ , then it follows from (4.16) that

$$\begin{aligned}
& \lim_{\gamma \rightarrow 1^+} \int_0^{+\infty} \int_{-\infty}^{+\infty} (\rho u + \rho^\gamma u) \left( \frac{x}{t} \right) \psi(x, t) dx dt \\
&= \lim_{\gamma \rightarrow 1^+} \int_0^{+\infty} t \left( \int_{-\infty}^{+\infty} (1 + \rho^{\gamma-1}(\xi)) \rho(\xi) u(\xi) \psi(\xi t, t) d\xi \right) dt \\
&= \int_0^{+\infty} t \left( \lim_{\gamma \rightarrow 1^+} \int_{-\infty}^{+\infty} (1 + \rho^{\gamma-1}(\xi)) \rho(\xi) u(\xi) \psi(\xi t, t) d\xi \right) dt \\
&= \int_0^{+\infty} t \left( \int_{-\infty}^{+\infty} 2(\rho_- u_- + (\rho_+ u_+ - \rho_- u_-) H(\xi - u_+)) \psi(\xi t, t) d\xi + 2\rho_- u_- (u_- - u_+) \psi(u_+ t, t) \right) dt \\
&= \int_0^{+\infty} t \left( \frac{1}{t} \int_{-\infty}^{+\infty} 2(\rho_- u_- + (\rho_+ u_+ - \rho_- u_-) H(\frac{x}{t} - u_+)) \psi(x, t) dx + 2\rho_- u_- (u_- - u_+) \psi(u_+ t, t) \right) dt \\
&= \int_0^{+\infty} \int_{-\infty}^{+\infty} 2(\rho_- u_- + (\rho_+ u_+ - \rho_- u_-) H(x - u_+ t)) \psi(x, t) dx dt + \int_0^{+\infty} 2\rho_- u_- (u_- - u_+) t \psi(u_+ t, t) dt,
\end{aligned}$$

which permits us to get the desired result (4.12). To be more precise, it can be further obtained that

$$\begin{aligned}
& \lim_{\gamma \rightarrow 1^+} \int_0^{+\infty} \int_{-\infty}^{+\infty} \rho u \left( \frac{x}{t} \right) \psi(x, t) dx dt \\
&= \int_0^{+\infty} \int_{-\infty}^{+\infty} (\rho_- u_- + (\rho_+ u_+ - \rho_- u_-) H(x - u_+ t)) \psi(x, t) dx dt + \int_0^{+\infty} \rho_- u_+ (u_- - u_+) t \psi(u_+ t, t) dt,
\end{aligned}$$

and

$$\begin{aligned}
& \lim_{\gamma \rightarrow 1^+} \int_0^{+\infty} \int_{-\infty}^{+\infty} \rho^\gamma u \left( \frac{x}{t} \right) \psi(x, t) dx dt \\
&= \int_0^{+\infty} \int_{-\infty}^{+\infty} (\rho_- u_- + (\rho_+ u_+ - \rho_- u_-) H(x - u_+ t)) \psi(x, t) dx dt + \int_0^{+\infty} \rho_- (u_- - u_+) (2u_- - u_+) t \psi(u_+ t, t) dt,
\end{aligned}$$

On the other hand, it can also be deduced from (4.17) that

$$\begin{aligned}
\lim_{\gamma \rightarrow 1^+} \int_0^{+\infty} \int_{-\infty}^{+\infty} \rho \left( \frac{x}{t} \right) \psi(x, t) dx dt &= \int_0^{+\infty} \int_{-\infty}^{+\infty} (\rho_- + (\rho_+ - \rho_-) H(x - u_+ t)) \psi(x, t) dx dt \\
&\quad + \int_0^{+\infty} \rho_- (u_- - u_+) t \psi(u_+ t, t) dt,
\end{aligned}$$

which gives rise to the expected result (4.11). This ends the proof.  $\square$

Let us turn our attention to investigate the limiting behavior  $\gamma \rightarrow 1^+$  of Riemann solution of (1.2)–(1.3) in the case of  $u_+ > u_- > 0$ , which can be illustrated well in the following theorem.

**Theorem 4.3.** *Suppose that  $\gamma - 1 (> 0)$  is taken small enough, then the Riemann solution of (1.2)–(1.3) consists of 1-rarefaction wave  $R_1$  and 2-contact discontinuity  $J_2$  with the intermediate non-vacuum constant state when*

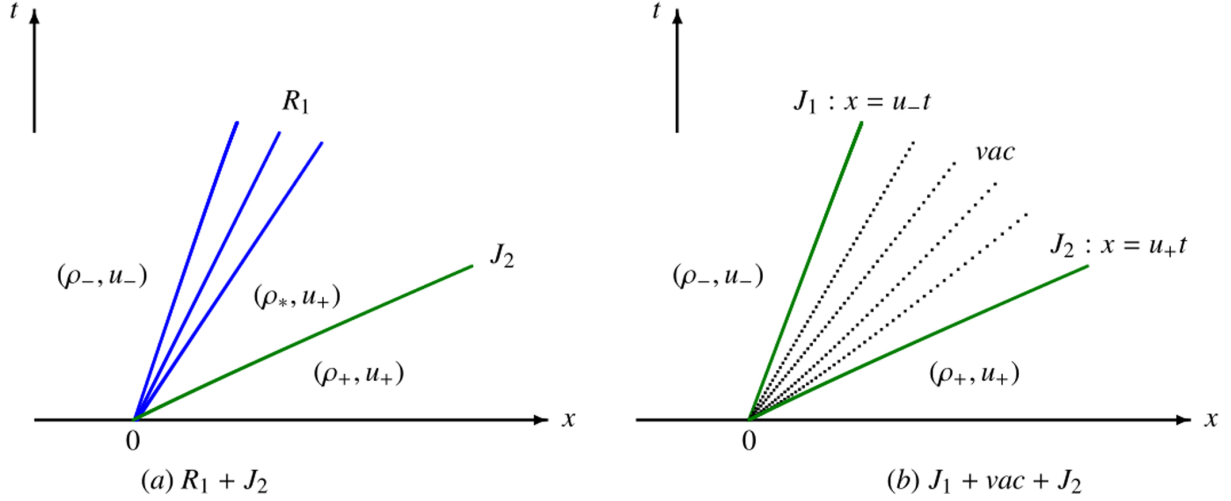


FIGURE 3. In the case of  $u_- < u_+ < 2u_-$ , the Riemann solution of (1.2)–(1.3) consists of a 1-rarefaction wave  $R_1$  and a 2-contact discontinuity  $J_2$  with the non-vacuum intermediate state  $(\rho_*, u_+)$  for  $\gamma - 1 (> 0)$  sufficiently small on the left-hand side. In the limiting  $\gamma \rightarrow 1^+$  situation, the wave-front of  $R_1$  coincides with the front of  $J_2$  as well as the state inside the interior of  $R_1$  becomes vacuum gradually on the right-hand side.

$u_- < u_+ < 2u_-$  or the vacuum intermediate state when  $u_+ > 2u_-$ . In the limiting  $\gamma \rightarrow 1^+$  situation, the state in the interior of the 1-rarefaction wave fan  $R_1$  is transformed into vacuum. Moreover, the limit  $\gamma \rightarrow 1^+$  of Riemann solution of (1.2)–(1.3) is well consistent with the corresponding solution (2.1) of the Riemann problem (1.4) and (1.3).

*Proof.* It is evident to know from Section 3 that the Riemann solution of (1.2)–(1.3) consists of a 1-rarefaction wave  $R_1$  and a 2-contact discontinuity  $J_2$  accompanied with the non-vacuum intermediate state when  $u_- < u_+ < u_-(1 + \rho_-^{\gamma-1})$  (see Fig. 3a) or the vacuum intermediate state when  $u_+ > u_-(1 + \rho_-^{\gamma-1})$  (see Fig. 4a). In other words, the vacuum state appears or not depending on the ordering relation between  $\bar{u} = u_-(1 + \rho_-^{\gamma-1})$  and  $u_+$ . It suffices to get

$$\lim_{\gamma \rightarrow 1^+} \bar{u} = \lim_{\gamma \rightarrow 1^+} u_-(1 + \rho_-^{\gamma-1}) = 2u_-. \quad (4.18)$$

Thus, if  $u_- < u_+ < 2u_-$ , then the vacuum state cannot appear in the Riemann solution of (1.2)–(1.3) when  $\gamma - 1$  is taken to be a sufficiently small positive number. Otherwise, if  $u_+ > 2u_-$ , then the vacuum state is certainly presented in the Riemann solution of (1.2)–(1.3) by taking  $\gamma - 1 (> 0)$  small enough. As a consequence, we need to deal with our limiting problem by taking into account two different cases according to  $u_+ < 2u_-$  or not.

On the one hand, for the case  $u_- < u_+ < 2u_-$ , we can take  $\gamma - 1 (> 0)$  sufficiently small, such that it suffices to get  $u_- < u_+ < u_-(1 + \rho_-^{\gamma-1})$ . In this situation, the Riemann solution of (1.2)–(1.3) can be expressed as  $R_1 + J_2$  given by (3.15). It is evident to find that the following inequality

$$0 < \lim_{\gamma \rightarrow 1^+} \frac{(1 + \rho_-^{\gamma-1})u_- - u_+}{u_+} = \frac{2u_- - u_+}{u_+} < 1 \quad (4.19)$$

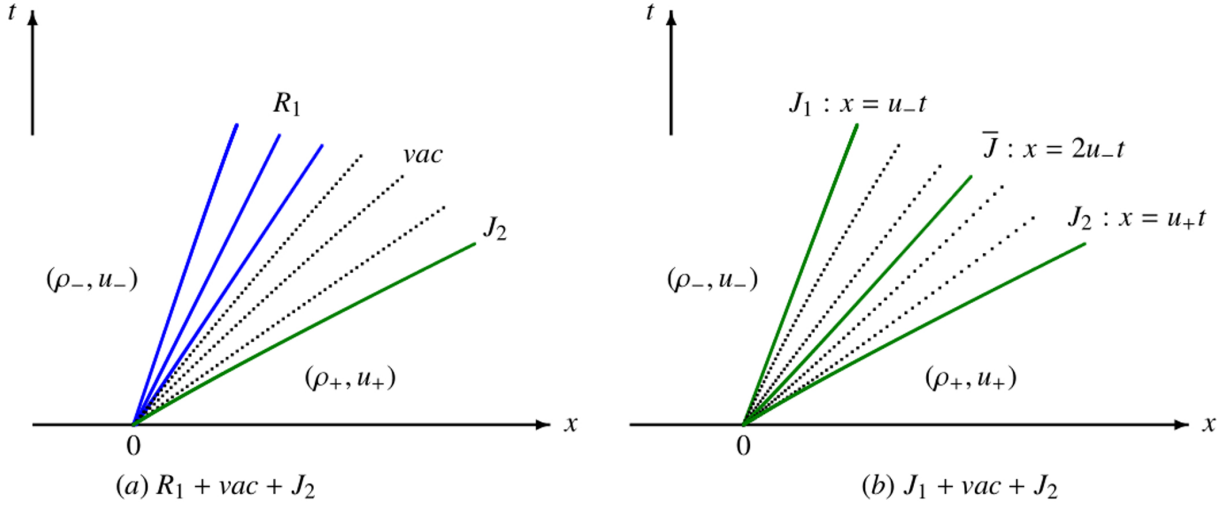


FIGURE 4. In the case of  $u_+ > 2u_-$ , the Riemann solution of (1.2)–(1.3) consists of a 1-rarefaction wave  $R_1$  and a 2-contact discontinuity  $J_2$  with the vacuum intermediate state by taking  $\gamma - 1 (> 0)$  small enough on the left-hand side. Then, the wave-front of  $R_1$  tends to the line  $\bar{J} : x = 2u_-t$  as  $\gamma \rightarrow 1^+$ . In the limiting  $\gamma \rightarrow 1^+$  situation, the state inside the interior of  $R_1$  also becomes vacuum as well as the region between the fronts of  $\bar{J}$  and  $J_2$  is also covered by the vacuum state on the right-hand side.

holds now when  $u_- < u_+ < 2u_-$ . By (3.13), it holds that

$$\lim_{\gamma \rightarrow 1^+} \rho_* = \lim_{\gamma \rightarrow 1^+} \left( \frac{2u_- - u_+}{u_+} \right)^{\frac{1}{\gamma-1}} = 0, \quad (4.20)$$

which implies that the intermediate state  $(\rho_*, u_+)$  becomes the vacuum state  $(0, u_+)$  in the limiting  $\gamma \rightarrow 1^+$  situation. It can be derived from the second equation in (3.18) together with (3.13) that

$$\lambda_1(\rho_*, u_+) = \left( \frac{(2 - \gamma)u_-(1 + \rho_-^{\gamma-1}) + (\gamma - 1)u_+}{u_-(1 + \rho_-^{\gamma-1})} \right) u_+. \quad (4.21)$$

Therefore, sending the limits  $\gamma \rightarrow 1^+$  in the first equation of (3.18) and (4.21) respectively gives

$$\lim_{\gamma \rightarrow 1^+} \lambda_1(\rho_-, u_-) = \lim_{\gamma \rightarrow 1^+} \frac{(1 + (2 - \gamma)\rho_-^{\gamma-1})u_-}{1 + \rho_-^{\gamma-1}} = u_-, \quad (4.22)$$

$$\lim_{\gamma \rightarrow 1^+} \lambda_1(\rho_*, u_+) = \lim_{\gamma \rightarrow 1^+} \left( \frac{(2 - \gamma)u_-(1 + \rho_-^{\gamma-1}) + (\gamma - 1)u_+}{u_-(1 + \rho_-^{\gamma-1})} \right) u_+ = u_+. \quad (4.23)$$

This means that the wave back of  $R_1$  tends to the line  $x = u_-t$  as well as the wave front of  $R_1$  tends to the line  $x = u_+t$  in the limiting  $\gamma \rightarrow 1^+$  situation. It is of interest to find in the limiting  $\gamma \rightarrow 1^+$  situation that the wave front of  $R_1$  is coincident with that of  $J_2$ , such that the middle region between the wave front of  $R_1$  and  $J_2$  disappears although the state  $(\rho_*, u_+)$  in this middle region also becomes the vacuum state  $(0, u_+)$ .

In the current position, we have no choice but to study elaborately all the states  $(\rho, u)$  in the interior of 1-rarefaction wave fan. For a fixed point  $(x, t)$  in the interior of  $R_1$ , it is obvious to see that the following inequality

$$u_- < \xi = \frac{x}{t} < u_+ < 2u_-$$

holds in the limiting  $\gamma \rightarrow 1^+$  situation, which allows us to get

$$0 < \frac{2u_-t}{x} - 1 < 1. \quad (4.24)$$

In addition, it follows from (3.16) that

$$\frac{x}{t} = \frac{(1 + (2 - \gamma)\rho^{\gamma-1})(1 + \rho_-^{\gamma-1})u_-}{(1 + \rho^{\gamma-1})^2}, \quad (4.25)$$

and also

$$\frac{x}{t} = \left( \frac{(2 - \gamma)(1 + \rho_-^{\gamma-1})u_- + (\gamma - 1)u}{(1 + \rho_-^{\gamma-1})u_-} \right) u, \quad (4.26)$$

in which  $0 < \rho < \rho_-$  and  $u_- < u < u_+ < 2u_-$ . With  $(x, t)$  being fixed in the interior of  $R_1$ , sending the limit  $\gamma \rightarrow 1^+$  in (4.25) and (4.26) yields

$$\lim_{\gamma \rightarrow 1^+} \rho^{\gamma-1} = \frac{2u_-t}{x} - 1 \quad \text{and} \quad \lim_{\gamma \rightarrow 1^+} u(x, t) = \frac{x}{t}. \quad (4.27)$$

Taking into account (4.24), it can be derived obviously from the first equation of (4.27) that

$$\lim_{\gamma \rightarrow 1^+} \rho(x, t) = \lim_{\gamma \rightarrow 1^+} \left( \frac{2u_-t}{x} - 1 \right)^{\frac{1}{\gamma-1}} = 0. \quad (4.28)$$

In a word, in the case of  $u_- < u_+ < 2u_-$ , the wave-front of  $R_1$  coincides with the front of  $J_2$  as well as the state inside the interior of  $R_1$  becomes the corresponding vacuum state with the virtual velocity  $u = \frac{x}{t}$  in the limiting  $\gamma \rightarrow 1^+$  situation (see Fig. 3b), which is exactly the same as the solution (2.1) of the Riemann problem (1.4) and (1.3).

On the other hand, for the case  $u_+ > 2u_-$ , we can also take  $\gamma - 1 (> 0)$  small enough, such that  $u_+ > u_-(1 + \rho_-^{\gamma-1})$  holds now. In this situation, the Riemann solution of (1.2)–(1.3) can be written as  $R_1 + vac + J_2$  given by (3.19). As before, we can also arrive at (4.22) and

$$\lim_{\gamma \rightarrow 1^+} \lambda_1(0, \bar{u}) = \lim_{\gamma \rightarrow 1^+} \bar{u} = \lim_{\gamma \rightarrow 1^+} u_-(1 + \rho_-^{\gamma-1}) = 2u_-. \quad (4.29)$$

This indicates that the velocities of wave-back and wave-front of  $R_1$  converge to  $u_-$  and  $2u_-$  as  $\gamma \rightarrow 1^+$ , respectively. Similarly, we need to study all the states  $(\rho, u)$  in the interior of 1-rarefaction wave fan. For a fixed point  $(x, t)$  in the interior of  $R_1$ , the following inequality

$$u_- < \xi = \frac{x}{t} < 2u_- < u_+$$

is true in the limiting  $\gamma \rightarrow 1^+$  situation, which also permits one to get (4.24). With the same argument as before, we also arrive at (4.27) and (4.28) by sending the limits  $\gamma \rightarrow 1^+$  in (4.25) and (4.26). All in all, in the case of  $u_+ > 2u_-$ , the state inside the interior of  $R_1$  is also changed into the corresponding vacuum state with the virtual velocity  $u = \frac{x}{t}$  in the limiting  $\gamma \rightarrow 1^+$  situation. Simultaneously, the region between the fronts of  $\bar{J}$  and  $J_2$  is also covered by the vacuum state in the limiting  $\gamma \rightarrow 1^+$  situation as before (see Fig. 4b). Hence, the limit  $\gamma \rightarrow 1^+$  of Riemann solution  $R_1 + vac + J_2$  of (1.2)–(1.3) for the case  $u_+ > 2u_-$  is also in agreement with the solution (2.1) of the Riemann problem (1.4) and (1.3). The proof is completed by gathering the two different cases together.  $\square$

## 5. NUMERICAL SIMULATIONS FOR $\delta$ -SHOCK AND VACUUM

In this section, some representative numerical results are presented for the Riemann solutions of (1.2)–(1.3) to give the exact description of the formation process of  $\delta$ -shock and vacuum mentioned in Section 4. Thereinafter, we consider the following three different typical cases of Riemann initial data:

$$u_- > u_+, \quad 2u_- > u_+ > u_-, \quad u_+ > 2u_-.$$

Many more numerical tests have also been performed to make sure that the obtained results displayed in the current work are not numerical artifacts. Based on split-coefficient matrix method (SCMM) [19], we employ the first order upwind scheme to discretize the system (1.2). We now convert (1.2) into the following quasi-linear form:

$$U_t + AU_x = 0,$$

in which

$$U = \begin{pmatrix} \rho \\ u \end{pmatrix} \quad \text{and} \quad A = \begin{pmatrix} u & \rho \\ 0 & \frac{(1 + (2 - \gamma)\rho^{\gamma-1})u}{1 + \rho^{\gamma-1}} \end{pmatrix}.$$

Furthermore, one has  $A = R\Lambda L$ , where

$$R = \begin{pmatrix} 1 + \rho^{\gamma-1} & 1 \\ (1 - \gamma)\rho^{\gamma-2}u & 0 \end{pmatrix}, \quad \Lambda = \begin{pmatrix} \lambda_1 & 0 \\ 0 & \lambda_2 \end{pmatrix}, \quad L = \begin{pmatrix} 0 & \frac{1}{(1 - \gamma)\rho^{\gamma-2}u} \\ 1 & \frac{1 + \rho^{\gamma-1}}{(\gamma - 1)\rho^{\gamma-2}u} \end{pmatrix}.$$

Based on the SCMM, the first order upwind scheme can be written as

$$U_j^{n+1} = U_j^n - \frac{\Delta t}{\Delta x} \{A_j^- (U_{j+1}^n - U_j^n) + A_j^+ (U_j^n - U_{j-1}^n)\},$$

where

$$A_j^+ = \frac{A_j^n + |A_j^n|}{2}, \quad A_j^- = \frac{A_j^n - |A_j^n|}{2} \quad \text{and} \quad |A| = R_j^n |\Lambda_j^n| L_j^n.$$

In the following numerical simulations, as in [1, 2], we shall take the same initial data to observe the formation of  $\delta$ -shock and vacuum from the Riemann solutions of (1.2)–(1.3) under the different  $\gamma$ -values given by  $\gamma = 1.5, 1.1, 1.01$ . For the case  $u_- > u_+$ , we take the following initial data:

$$\text{Data 1:} \quad \rho_- = 0.35, \quad u_- = 0.4, \quad \rho_+ = 0.25, \quad u_+ = 0.25, \quad (5.1)$$

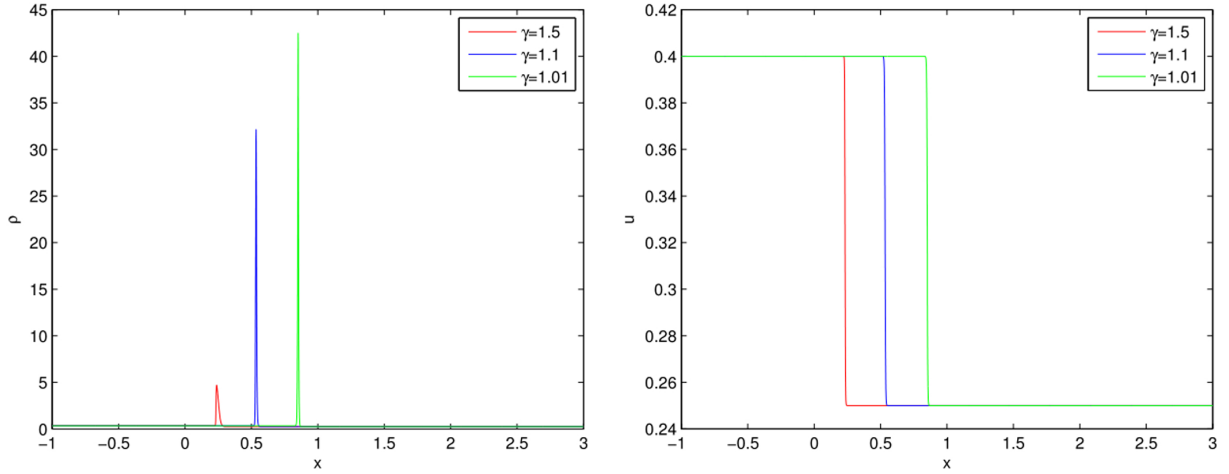


FIGURE 5. Numerical results for  $\rho$  and  $u$  are displayed respectively for the Riemann solution of (1.2)–(1.3) in the case of  $u_- > u_+ > 0$  by taking the detailed initial data (5.1) at the time  $t = 1$ .

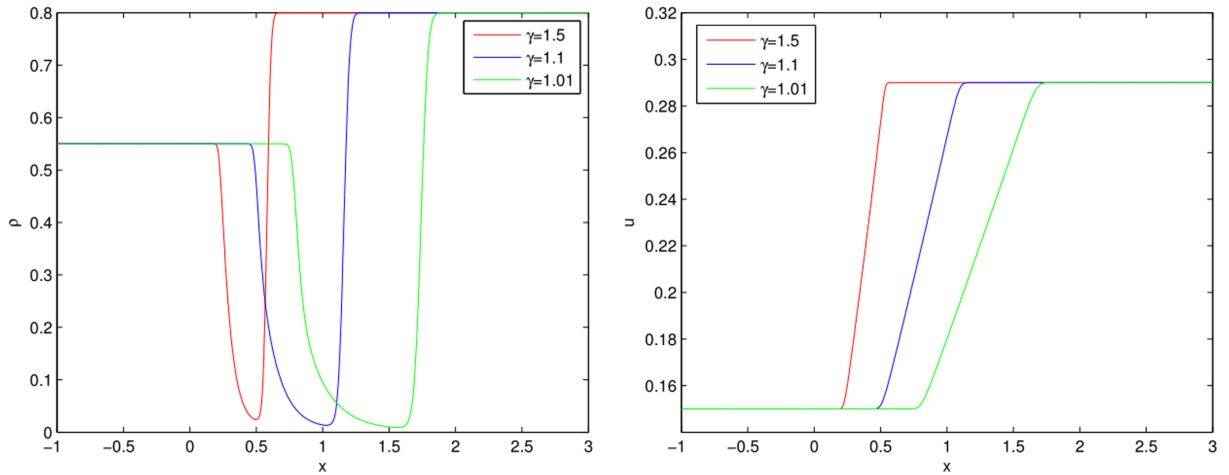


FIGURE 6. Numerical results for  $\rho$  and  $u$  are displayed respectively for the Riemann solution of (1.2)–(1.3) in the case of  $2u_- > u_+ > u_-$  by taking the initial data (5.2) at the time  $t = 2$ .

and present the numerical results at  $t = 1$  in Figure 5. It is shown that  $\rho$  has a sudden jump to indicate Dirac  $\delta$ -function developed at the position of  $\delta$ -shock front as  $\gamma$  tends to 1, which is in accordance with Theorem 4.2. In addition,  $u$  is a  $L^\infty(R_+^2; R)$  function, which is also consistent with the result in (4.10).

For the case  $2u_- > u_+ > u_-$ , we take the initial data as below:

$$\text{Data 2: } \rho_- = 0.55, \quad u_- = 0.15, \quad \rho_+ = 0.8, \quad u_+ = 0.29, \quad (5.2)$$

and present the numerical results at  $t = 2$  in Figure 6. It is shown that  $\rho(x, t)$  goes from  $\rho_-$  to  $\rho_*$  by a continuous function and then  $\rho$  goes from  $\rho_*$  to  $\rho_+$  by a  $L^\infty(R_+^2; R)$  function. The state variable  $\rho(x, t)$  in wave fan of  $R_1$  and  $\rho_*$  tend to 0 as  $\gamma$  tends to 1, which is in accordance with (4.28). In addition,  $u(x, t)$  changes from  $u_-$  to  $u_+$  by a continuous function, which is also consistent with the result in (4.27).

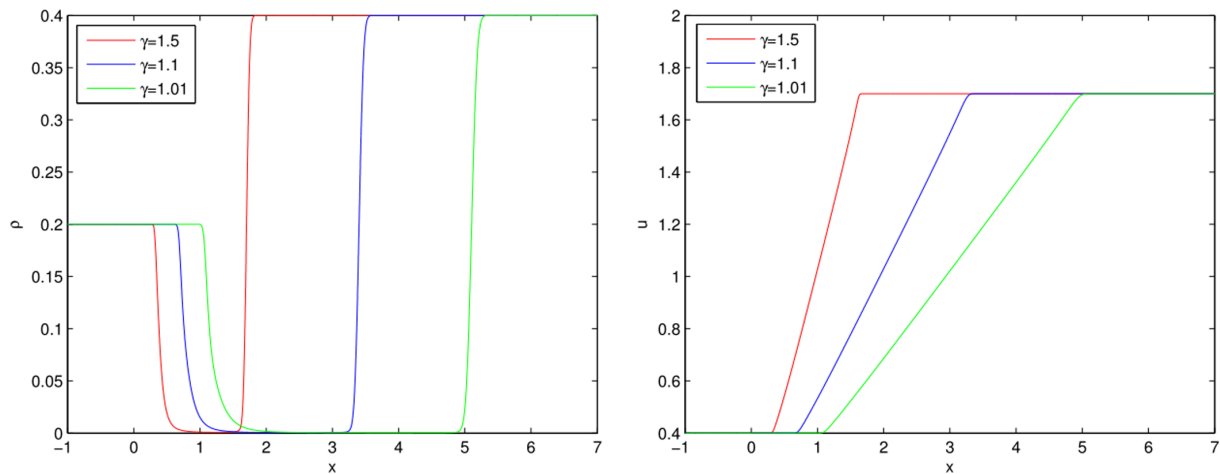


FIGURE 7. Numerical results for  $\rho$  and  $u$  are displayed respectively for the Riemann solution of (1.2)–(1.3) in the case of  $u_+ > 2u_-$  by taking the initial data (5.3) at the time  $t = 1$ .

To the end, for the case  $u_+ > 2u_-$ , we take the initial data as follows:

$$\text{Data 3: } \rho_- = 0.2, \quad u_- = 0.4, \quad \rho_+ = 0.4, \quad u_+ = 1.7, \quad (5.3)$$

and present the numerical results at  $t = 1$  in Figure 7. It is shown that  $\rho(x, t)$  goes from  $\rho_-$  to 0 by a continuous function and then  $\rho$  goes from 0 to  $\rho_+$  by a  $L^\infty(R_+^2; R)$  function. The state variable  $\rho(x, t)$  in the wave fan of  $R_1$  tends to 0 as  $\gamma$  tends to 1, which is in accordance with (4.28). In addition,  $u(x, t)$  changes from  $u_-$  to  $u_+$  by a continuous function, which is also consistent with the result in (4.27).

As a result, under the condition  $u_- > u_+ > 0$ , the state variable  $\rho$  has an impulse at the specific position  $x = u_+t$ , which implies that Dirac  $\delta$ -function is developed gradually for the state variable  $\rho$  in the Riemann solution of (1.2)–(1.3) at the position of  $\delta$ -shock front during the limiting  $\gamma \rightarrow 1^+$  process. On the other hand, the vacuum state between two contact discontinuities is also formed in the Riemann solution of (1.2)–(1.3) during the limiting  $\gamma \rightarrow 1^+$  process when the condition  $u_+ > u_- > 0$  is satisfied. It is interesting to see that the above numerical solutions are very close to our theoretical derivations under some appropriate initial data. As a consequence, we can conclude that these numerical results are in complete agreement with our theoretical analysis in Section 4.

*Acknowledgements.* The authors are very grateful to the three anonymous referees for their very helpful comments which improve the original manuscript greatly. This work is supported in part by Shandong Provincial Natural Science Foundation (ZR2019MA058).

## REFERENCES

- [1] E. Abreu, R. De la Cruz and W. Lambert, Riemann problem and delta-shock solutions for a Keyfitz-Kranzer system with a forcing term. *J. Math. Anal. Appl.* **502** (2021) 125267.
- [2] A. Aggarwal, G. Vaidya and G.D.V. Gowda, Positivity-preserving numerical scheme for hyperbolic systems with delta-shock solutions and its convergence analysis. *Z. Angew. Math. Phys.* **72** (2021) 165.
- [3] D. Armbruster and M. Wienke, Kinetic models and intrinsic timescales: simulation comparison for a 2nd order queueing model. *Kinetic Related Models* **12** (2019) 177–193.
- [4] D. Armbruster, D. Marthaler and C. Ringhofer, Kinetic and fluid model hierarchies for supply chains. *Multiscale Model. Simul.* **2** (2013) 43–61.
- [5] D. Armbruster, P. Degond and C. Ringhofer, A model for the dynamics of large queueing networks and supply chains. *SIAM J. Appl. Math.* **66** (2006) 896–920.

- [6] F. Betancourt, R. Burger, C. Chalons, S. Diehl and S. Faras, A random sampling approach for a family of Temple-class systems of conservation laws. *Numer. Math.* **138** (2018) 37–73.
- [7] F. Bouchut, On zero pressure gas dynamics, in vol. 22 of *Advances in Kinetic Theory and Computing, Ser. Adv. Math. Appl. Sci.* World Sci. Publishing, River Edge, NJ (1994) 171–190.
- [8] G.Q. Chen and H. Liu, Formation of  $\delta$ -shocks and vacuum states in the vanishing pressure limit of solutions to the Euler equations for isentropic fluids. *SIAM J. Math. Anal.* **34** (2003) 925–938.
- [9] V.G. Danilov and V.M. Shelkovich, Dynamics of propagation and interaction of  $\delta$ -shock waves in conservation law systems. *J. Differ. Equ.* **211** (2005) 333–381.
- [10] L. Forestier-Coste, S. Gottlich and M. Herty, Data-fitted second-order macroscopic production models. *SIAM J. Appl. Math.* **75** (2015) 999–1014.
- [11] L. Guo, T. Li and G. Yin, The vanishing pressure limits of Riemann solutions to the Chaplygin gas equations with a source term. *Commun. Pure Appl. Anal.* **16** (2017) 295–309.
- [12] L. Guo, T. Li and G. Yin, The transition of Riemann solutions of the modified Chaplygin gas equations with friction to the solutions of the Chaplygin gas equations. *Z. Angew. Math. Mech.* **102** (2022) e201800064.
- [13] S.T. Hilden, H.M. Nilsen and X. Raynaud, Study of the well-posedness of models for the inaccessible pore volume in polymer flooding. *Transport in Porous Media* **114** (2016) 65–86.
- [14] F. Huang and Z. Wang, Well-posedness for pressureless flow. *Comm. Math. Phys.* **222** (2001) 117–146.
- [15] M. Ibrahim, F. Liu and S. Liu, Concentration of mass in the pressureless limit of Euler equations for power law. *Nonlinear Analysis: RWA* **47** (2019) 224–235.
- [16] H. Kalisch and D. Mitrovic, Singular solutions of a fully nonlinear  $2 \times 2$  system of conservation laws. *Proc. Edinburgh Math. Soc.* **55** (2012) 711–729.
- [17] H. Kalisch, D. Mitrovic and V. Teyekpiti, Existence and uniqueness of singular solutions for a conservation law arising in magnetohydrodynamics. *Nonlinearity* **31** (2018) 5463–5483.
- [18] H. Kalisch, D. Mitrovic and V. Teyekpiti, Delta shock waves in shallow water flow. *Phys. Lett. A* **381** (2017) 1138–1144.
- [19] D.M. Lu, H.C. Simpson and A. Gilchrist, The application of split-coefficient matrix method to transient two phase flows. *Int. J. Num. Meth. Heat Fluid flow* **6** (1996) 63–76.
- [20] M. Mazzotti, A. Tarafder, J. Cornel, F. Gritti and G. Guiochon, Experimental evidence of a delta-shock in nonlinear chromatography. *J. Chromatogr. A* **1217** (2010) 2002–2012.
- [21] T. Minhajul and R. Sekhar, Nonlinear wave interactions in a macroscopic production model. *Acta Math. Sci. Ser. B* **41** (2021) 764–780.
- [22] D. Mitrovic and M. Nedeljkov, Delta-shock waves as a limit of shock waves. *J. Hyperbolic Differ. Equ.* **4** (2007) 629–653.
- [23] M. Nedeljkov, Shadow waves: entropies and interactions for delta and singular shocks. *Arch. Rational Mech. Anal.* **197** (2010) 489–537.
- [24] A. Qu, H. Yuan and Q. Zhao, High Mach number limit of one-dimensional piston problem for non-isentropic compressible Euler equations: polytropic gas. *J. Math. Phys.* **61** (2020) 011507.
- [25] C.O.R. Sarrico and A. Paiva, Delta shock waves in the shallow water system. *J. Dyn. Differ. Equ.* **30** (2018) 1187–1198.
- [26] A. Sen and T. Raja Sekhar, The limiting behavior of the Riemann solution to the isentropic Euler system for the logarithmic equation of state with a source term. *Math. Methods Appl. Sci.* **44** (2021) 7207–7207.
- [27] A. Sen and T. Raja Sekhar, Delta shock wave as self-similar viscosity limit for a strictly hyperbolic system of conservation laws. *J. Math. Phys.* **60** (2019) 051510.
- [28] A. Sen and T. Raja Sekhar, Delta shock wave and wave interactions in a thin film of a perfectly soluble anti-surfactant solution. *Commun. Pure Appl. Anal.* **19** (2020) 2641–2653.
- [29] A. Sen, T. Raja Sekhar and D. Zeidan, Stability of the Riemann solution for a  $2 \times 2$  strictly hyperbolic system of conservation laws. *Sadhana* **44** (2019) 228.
- [30] C. Shen and M. Sun, Formation of delta shocks and vacuum states in the vanishing pressure limit of Riemann solutions to the perturbed Aw-Rascle model. *J. Differ. Equ.* **249** (2010) 3024–3051.
- [31] C. Shen and M. Sun, Exact Riemann solutions for the drift-flux equations of two-phase flow under gravity. *J. Differ. Equ.* **314** (2022) 1–55.
- [32] W. Sheng and T. Zhang, The Riemann problem for the transportation equations in gas dynamics. *Mem. Amer. Math. Soc.* **137** (N654) (1999) 1–77.
- [33] W. Sheng, G. Wang and G. Yin, Delta wave and vacuum state for generalized Chaplygin gas dynamics system as pressure vanishes. *Nonlinear Analysis: RWA* **22** (2015) 115–128.
- [34] S. Sheng and Z. Shao, The vanishing adiabatic exponent limits of Riemann solutions to the isentropic Euler equations for power law with a Coulomb-like friction term. *J. Math. Phys.* **60** (2019) 101504.
- [35] S. Sheng and Z. Shao, The limits of Riemann solutions to Euler equations of compressible fluid flow with a source term. *J. Engineering Math.* **125** (2020) 1–22.
- [36] S. Sheng and Z. Shao, Concentration of mass in the pressureless limit of the Euler equations of one-dimensional compressible fluid flow. *Nonlinear Analysis: RWA* **52** (2020) 103039.
- [37] S. Sil and T. Raja Sekhar, Nonlocally related systems, nonlocal symmetry reductions and exact solutions for one-dimensional macroscopic production model. *Eur. Phys. J. Plus* **135** (2020) 514.
- [38] S. Sil and T. Raja Sekhar, Nonclassical symmetry analysis, conservation laws of one-dimensional macroscopic production model and evolution of nonlinear waves. *J. Math. Anal. Appl.* **497** (2021) 124847.

- [39] M. Sun, Singular solutions to the Riemann problem for a macroscopic production model. *Z. Angew. Math. Mech.* **97** (2017) 916–931.
- [40] M. Sun, The limits of Riemann solutions to the simplified pressureless Euler system with flux approximation. *Math. Methods Appl. Sci.* **41** (2018) 4528–4548.
- [41] M. Sun, Concentration and cavitation phenomena of Riemann solutions for the isentropic Euler system with the logarithmic equation of state. *Nonlinear Analysis: RWA* **53** (2020) 103068.
- [42] B. Temple, Systems of conservation laws with invariant submanifolds. *Trans. Am. Math. Soc.* **280** (1983) 781–795.
- [43] P. Wang and C. Shen, The perturbed Riemann problem for a macroscopic production model with Chaplygin gas. *Bull. Malays. Math. Sci. Soc.* **44** (2021) 1195–1214.
- [44] H. Yang and J. Liu, Delta-shocks and vacuums in zero-pressure gas dynamics by the flux approximation. *Science China Math.* **58** (2015) 2329–2346.
- [45] H. Yang and Y. Zhang, Pressure and flux-approximation to the isentropic relativistic Euler equations for the modified Chaplygin gas. *J. Math. Phys.* **60** (2019) 071502.
- [46] Q. Zhang, Concentration in the flux approximation limit of Riemann solutions to the extended Chaplygin gas equations with friction. *J. Math. Phys.* **60** (2019) 101508.
- [47] Y. Zhang and M. Sun, The intrinsic phenomena of concentration and cavitation on the Riemann solutions for the perturbed macroscopic production model. *Math. Meth. Appl. Sci.* **45** (2022) 864–881.
- [48] Y. Zhang, Y. Zhang and J. Wang, Concentration in the zero-exponent limit of solutions to the isentropic Euler equations for extended Chaplygin gas. *Asymptotic Anal.* **122** (2021) 35–67.
- [49] Y. Zhang, Y. Zhang and J. Wang, Zero-exponent limit to the extended Chaplygin gas equations with friction. *Bull. Malays. Math. Sci. Soc.* **44** (2021) 3571–3599.

## Subscribe to Open (S2O)

A fair and sustainable open access model



This journal is currently published in open access under a Subscribe-to-Open model (S2O). S2O is a transformative model that aims to move subscription journals to open access. Open access is the free, immediate, online availability of research articles combined with the rights to use these articles fully in the digital environment. We are thankful to our subscribers and sponsors for making it possible to publish this journal in open access, free of charge for authors.

### **Please help to maintain this journal in open access!**

Check that your library subscribes to the journal, or make a personal donation to the S2O programme, by contacting [subscribers@edpsciences.org](mailto:subscribers@edpsciences.org)

More information, including a list of sponsors and a financial transparency report, available at: <https://www.edpsciences.org/en/math-s2o-programme>